Journal of Theoretical and Applied Mechanics, Sofia, Vol. 47 No. 1 (2017) pp. 49-68
DE GRUYTER OPEN
DOI: 10.1515/jtam-2017-0004

A COMPUTATION FLUID DYNAMIC MODEL FOR GAS LIFT PROCESS SIMULATION IN A VERTICAL OIL WELL

ARASH KADIVAR, EBRAHIM NEMATI LAY*

Department of Chemical Engineering, Faculty of Engineering, University of Kashan, Kashan, Iran

[Received 30 November 2015. Accepted 20 March 2017]

ABSTRACT: Continuous gas-lift in a typical oil well was simulated using computational fluid dynamic (CFD) technique. A multi fluid model based on the momentum transfer between liquid and gas bubbles was employed to simulate two-phase flow in a vertical pipe. The accuracy of the model was investigated through comparison of numerical predictions with experimental data. The model then was used to study the dynamic behaviour of the two-phase flow around injection point in details. The predictions by the model were compared with other empirical correlations, as well. To obtain an optimum condition of gas-lift, the influence of the effective parameters including the quantity of injected gas, tubing diameter and bubble size distribution were investigated. The results revealed that increasing tubing diameter, the injected gas rate and decreasing bubble diameter improve gas-lift performance.

KEY WORDS: Continuous gas lift, two-phase flow, computational fluid dynamic (CFD), optimization.

1. INTRODUCTION

To meet the ever-increasing global demand of non renewable resources, the oil and gas industry is forced to rationalize and optimize its production and consumption. Majorities of the oil wells flow naturally in the early years of their lifetime. The well is not able to flow to the surface by passing the time and decreasing the driving force. Continuous gas lift, as one of the most economic artificial lift methods, has been always a point of interest to researchers led to more effective use of oil resources. In this process, the injection of high pressure natural gas into the wellbore leads to lighten the column of fluid and allows the reservoir pressure to flow the fluid to the surface [1]. The process was sketched in Fig. 1.

Determining the optimal operational conditions in gas lift process has been intensively studied in many papers. The initial step of gas lifting optimization was taken by Mayhill, developing the first correlation to formulate gas lift performance [2]. Gomez continued Mayhill study and introduced a two order one [3]. Kanu et al. optimized

*Corresponding author e-mail: enemati@kashanu.ac.ir

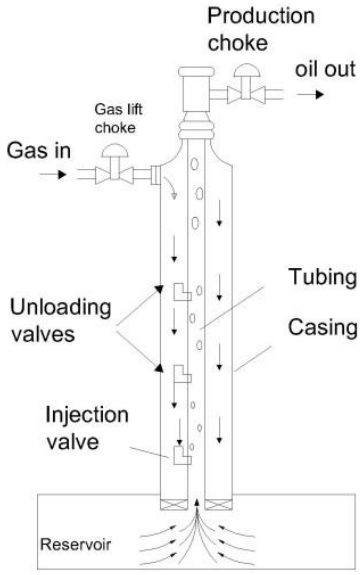

Fig. 1. Schematic of the continuous gas lift process.

the gas lift process economically through a new graphical method [4]. Mahmudi and Sadeghi [5] used an integrated mathematical model to design and operate a gas lift system. Moreover several studies have been conducted on design and optimization of gas lift, using different techniques, involving linear programming (LP), non-linear programming (NLP), dynamic programming (DP)..., etc. [6,7].

In this work, a multi fluid model developed by CFD technique was used to simulate the behaviour of two-phase fluid. The CFD model has been powerful and efficient tool to understand the complex hydrodynamics and mechanisms of gas liquid two-phase flows and it has been successfully tried and tested in many researches, including the oil and the gas industry. The accuracy of the multi fluid model was investigated by means of comparison of calculated pressure drops with experimental and measured field data.

The multi fluid model was used to investigate the dynamic behaviour of two-phase flow around the injection point in a typical oil well under gas lift in the south of Iran. The calculated pressure drop as the dominant part of gas lift simulation was compared with other empirical or semi-empirical models (i.e. Kabir and Hasan, Orkiszewski, Aziz and Govier, Chierici and Sclocchi and Duns and Ros) [8-12]. To reach the optimum condition of gas lift process, the influence of operational parameters, including tubing diameter, injected gas rate and bubble size distribution was studied.

2. TWO-PHASE FLOW MODELLING

In this work, the CFD model was used to introduce a procedure for the analysis of two-phase flow in a continuous gas lift system. A multiphase flow has been expressed, using its governing equations. The multiphase flow considered in this study consists of liquid as continuous phase ($q = l$) and gas as dispersed phases ($q = g$). By neglecting mass transfer between phases as well as assuming incompressible isothermal multiphase flow, the governing equations can be written as [13]:

Conservation of mass:

$$\frac{\partial(\alpha_q \rho_q)}{\partial t} + \nabla \cdot (\alpha_q \rho_q U_q) = 0\,. \tag{1}$$

Conservation of Momentum:

$$\begin{aligned} &\frac{\partial(\alpha_q \rho_q U_q)}{\partial t} + \nabla \cdot (\alpha_q \rho_q U_q U_q) \\ &\quad = -\alpha_q \nabla \cdot p_q + \alpha_q \rho_q g + \nabla \cdot (\alpha_q (S_q + S_q^{Re})) + (p_i - P_q)\nabla \cdot \alpha_q + F_q\,, \end{aligned} \tag{2}$$

where g, p_i, α_q and ρ_q are the gravitational acceleration, the interfacial pressure, the volume fraction and the density of phase q, respectively. U_q, p_q and S_qa re mean velocity, pressure and viscous stress of phase q. The unknown terms including interfacial force density, (F_q), Reynolds stresses of phase q, (S_q) and interfacial pressure difference, $(p_i - P_q)$, which arise from averaging of the instantaneous momentum equation and require modelling.

2.1. INTERFACIAL PRESSURE DIFFERENCE

Lamb considered the potential flow around single phase and expressed interfacial pressure difference, as follows [14]:

$$p_i - P_q = -C_p \rho_c |U_r|^2 \alpha_c\,, \tag{3}$$

where $C_p = 0.25$, $|U_r|$ is the relative velocity and ρ_c and α_c are density and void fraction of continuous phase, respectively. Drew pointed out, that by assumption of incompressible phases and without expansion or contraction there is microscopic instantaneous pressure equilibrium, i.e., $C_p = 0$ [15].

2.2. INTERFACIAL FORCES

For bubbly flow in pipes, the interfacial force acting on a dispersed phase is decomposed into several terms, expressed as

$$F_d = F_d^{drag} + F_d^{lift} + F_d^{wall} + F_d^{td} + F_d^{vm}. \tag{4}$$

The components of interfacial force density are drag, lift, wall, turbulence dispersion and virtual mass, respectively. It was assumed that in bubbly flow regime the interfacial force between dispersed phases were neglected [16]. Therefore, by Newton's law the interfacial force acting on continuous phase is

$$F_d = -F_c \tag{5}$$

The drag force acting on the dispersed phase travelling steadily through the fluid is illustrated as [17]

$$F_d^{drag} = K_{lg}\left(U_l - U_g\right) , \tag{6}$$

$$K_{lg} = \frac{3}{4}\frac{C_D}{d}\alpha_g \rho_l , \tag{7}$$

where d is the bubble diameter of a dispersed phase and C_D is the drag coefficient and can be written by the Schiller and Naumann correlation [18].

$$C_D = \begin{cases} 24(1 + 0.15Re_d^{0.687})/Re_d & Re_d \leq 1000 \\ 0.44 & Re_d > 1000 \end{cases} \tag{8}$$

$$Re_d = \frac{d|U_r|}{\nu_l} , \tag{9}$$

where Re_d is the particle Reynolds number and ν_l is the liquid (as continuous phase) kinematics viscosity.

A bubble moving through a fluid that is in a shearing motion will be subjected to a lift force transverse to the direction of motion. In general, the lift force is expressed as [15]

$$F_d^{lift} = -C_L \alpha_g \rho_l U_r \times \left(\nabla \times U_g\right) , \tag{10}$$

where C_L is the lift coefficient. Different constant values are reported for this coefficient. In this study, the modified lift coefficient was used, based on the Tomiyama's correlation and achieved by Behbahani et al. [16,19].

$$C_L = C_L^{mod} C_{L,\text{Tomiyama}}, \tag{11}$$

$$C_L^{mod} = \begin{cases} 0.2 & Eo_d < 1.17 \\ 0.1 & 1.17 < Eo_d < 2.65 \\ 0.05 & 2.65 < Eo_d < Eo_{d,crit} = 6.06 \\ 0.13 & 6.06 < Eo_d < 9.5 \\ \dfrac{0.04(14.9 - Eo_d)}{5.4} + 0.09 & 9.5 < Eo_d < 14.9 \\ \dfrac{0.04(23.5 - Eo_d)}{8.6} + 0.05 & 14.9 < Eo_d < 23.5 \end{cases} \tag{12}$$

$$d_H = \left(\frac{\sigma Eo_d}{g(\rho_l - \rho_g)}\right)^{0.5}, \tag{13}$$

where Eo_d is the Eötvös number, σ is the surface tension coefficient and d_H is the long axis of a deformable bubble.

Liquid flow rate between bubble and wall is lower than that between bubble and outer flow. This hydrodynamic pressure difference is the origin of wall force. There are several models for wall force, which have been reported in the literature. Here, Tomiyama's model, which has been proposed for flow in pipe geometry with tuned wall force coefficient [16,19] was selected which has the following general form:

$$F_d^{wall} = C_W \frac{\rho_l d \alpha_g |U_r|^2}{2} \left[\frac{1}{y_W^2} - \frac{1}{(D - y_W)^2}\right] n_W \,, \tag{14}$$

where D is the tubing diameter, y_m is the distance from wall and n_W is the wall normal vector. The modified wall force coefficient, based on the Tomiyama's correlation, concluded by Behbahani et al. [16,19], was used in this study.

$$C_W = C_W^{mod} C_{W,\text{Tomiyama}} \,, \tag{15}$$

$$C_L^{mod} = \begin{cases} 0.1 & E_{od} < 1.17 \\ 0.05 & E_{od} > 1.17 \end{cases} \tag{16}$$

Different models are introduced to estimate the interfacial turbulent dispersion force. As the Favre averaged- drag (FAD) model leads to accurate predictions for bubbly flow in vertical pipes, the FAD model was used in this study, which can be written as [20]

$$F_d^{td} = -K_{lg} U_{dr} = K_{lg} \frac{D_{lg}^t}{pr_{lg}} \left(\frac{\nabla \alpha_l}{\alpha_l} - \frac{\nabla \alpha_g}{\alpha_g}\right), \tag{17}$$

where U_{dr} is a drift velocity, pr_{dc} is a dispersion Prandtl number equal to 0.75 [16], and D_{lg}^t is the turbulent diffusivity.

Another component, the virtual-mass force, is considered when bubbles accelerate. The virtual mass force is calculated by Drew [15]

$$F_d^{vm} = C_{vm}\alpha_g\rho_l\left(\frac{D_lU_l}{D_t} - \frac{D_gU_g}{D_t}\right), \tag{18}$$

where D_p/D_t is the material time derivation of each phase, both continuous and dispersed phase, and C_{vm} is the virtual mass constant and is equal to $C_{\nu m} = 0.5$.

2.3. TURBULENCE IN MULTI-PHASE MODELLING

For gas lift optimization, it is usually desired to operate in the bubbly flow regime [21]. Two-equation turbulence models have been commonly used for bubbly flow in the vertical pipes. Here, the k–ε model, introduced by Harlow and Nakayama [22] was used, where k is the turbulence kinetic energy and ε is the rate of dissipation of the turbulent energy.

$$\begin{aligned}\frac{\partial(\rho_l\alpha_lk_l)}{\partial t} + \nabla(\rho_l\alpha_lk_lU_l) =&\alpha_lT_l^{Re} : (\nabla U_l)\\ &- \nabla\left(\frac{\rho_l\nu_l^t}{pr^{KE}}\nabla k_l\right) - \rho_l\alpha_l\varepsilon_l + R_k\end{aligned} \tag{19}$$

$$\begin{aligned}\frac{\partial(\rho_l\alpha_l\varepsilon_l)}{\partial t} + \nabla(\rho_l\alpha_l\varepsilon_lU_l) =&\frac{\varepsilon}{k}\left(C_1\alpha_lT_l^{Re} : (\nabla U_l) - C_2\rho_l\alpha_l\varepsilon_l\right)\\ &- \nabla\left(\frac{\rho_l\nu_l^t}{pr^{DR}}\nabla\varepsilon_l\right) + R_\varepsilon\end{aligned} \tag{20}$$

Using the definition of the turbulent length scale the eddy viscosity, ν_c^t is written as

$$\nu_l^t = C_\mu\frac{k_l^2}{\varepsilon_l}, \tag{21}$$

where T_c^{Re} is the Reynold stress. The source terms, R_k and R_ε, were used based on BelF'dhila and Simonin's correlation [23]. The constants in Eqs (19), (20) and (21) take the values, given in Table 1 [13].

Table 1. The values of the constants in the k–ε model

C_μ	C_1	C_2	pr^{KE}	pr^{DR}
0.09	1.44	1.92	1.0	1.272

2.4. PRESSURE VELOCITY COUPLING

Here, the adopted PISO algorithm for two-phase flow developed by Issa and Oliveira was used for the pressure-velocity coupling [24,25]. It involves one predictor step and two corrector step. The steps of the algorithm are defined as:

1: The continuous phase momentum equation is solved

$$\left(A_0^l + \frac{\alpha_l \rho_l V}{\delta t}\right) u_{il}^* = H_l^n\left(u_{il}^*\right) - \alpha_l^P \sum B_{ji}^P \left[\Delta P^n\right]_j^P + F_q\left(u_{ig}^n - u_{il}^n\right) V + S_{ui}^c + \frac{\alpha_c \rho_c V}{\delta t} u_{ic}^n. \tag{22}$$

2: The dispersed phase momentum equation is solved

$$\left(A_0^g + \frac{\alpha_g \rho_g V}{\delta t} + F_q V\right) \overset{*}{u}_{ig} = H_g^n\left(u_{ig}^*\right) - \alpha_g^P \sum B_{ji}^P \left[\Delta P^n\right]_j^P + F_q u_{il}^* V + S_{ui}^l + \frac{\alpha \rho_d V}{\delta t} u_{il}^n. \tag{23}$$

Where "*", "p" and "n" denote intermediate value, considered phase and time (or iteration) level, respectively. The superscripts "P" for the cell-center and "f" for the face along direction $l = j$ were considered for the locations of variables were computed. The contribution of surrounding cells will be denoted as $H\left(\emptyset\right) = \sum_f A_f \emptyset_f$, with $A_0 = \sum_f A_f$. Also, all quantities were assumed to be located at cell-center. B_{ji} is the i-component of the area-vector along j-direction, B_f is the face area and V is the cell volume and S_u^k contains all terms not explicitly written.

3: The corrected pressure p' is assembled using the overall continuity equation. The pressure and velocities are updated based on Issa& Oliveira equations [26]

$$A_P^p p_P' = \sum A_f^p p_f' + S_u^p\,, \tag{24}$$

$$\left(\frac{\alpha_l \rho_l V}{\delta t}\right)\left(u_{il}^{n+1} - u_{il}^*\right) = -\alpha_l^p \sum B_i^P \left[\Delta P'\right]_j^P\,, \tag{25}$$

$$\left(\frac{\alpha_g \rho_g V}{\delta t} + F_q V\right)\left(u_{ig}^{n+1} - u_{ig}^*\right) = -\alpha_g^p \sum B_i^P \left[\Delta P'\right]_j^P\,, \tag{26}$$

$$P^{n+1} = P^n + P'\,. \tag{27}$$

In the same way, the fluxes, $F*$, are corrected and defined, as [27]

$$\begin{aligned} F_{fg}^{n+1} &= F_{fg}^* - A_{fg}^P \left[\Delta P'\right]_f^f\,, \\ F_{fl}^{n+1} &= F_{fl}^* - A_{fl}^P \left[\Delta P'\right]_f^f \end{aligned} \tag{28}$$

4: The turbulence quantities should be solved for k and ε. With new values of k and ε, liquid and gas effective viscosities are updated.

5: The void fraction is updated through dispersed phase continuity equation, which is solved implicitly.

$$\left(A_o^a + \frac{\rho_d V}{\delta t} + Max\left[-div\left(u_g\right), 0\right]\right)\alpha^* = H_a^n\left(\alpha^*\right) + Max\left[div\left(u_g\right), 0\right] + \frac{\rho_g V}{\delta t}\alpha^n \tag{29}$$

The solution will be advanced in time until the residuals of all the equations are smaller than a specified value.

3. Pressure drop calculation

The prediction of pressure drop for bubbly flow in the tubing is very important in the gas-lift. The overall pressure drop for gas-liquid flow can be written as the sum of three individual components, i. e., acceleration, gravitational and frictional pressure losses.

$$\frac{\partial p}{\partial x} = \left(\frac{\partial p}{\partial x}\right)_A + \left(\frac{\partial p}{\partial x}\right)_H + \left(\frac{\partial p}{\partial x}\right)_F \tag{30}$$

In the bubble flow regime, the gravitational component usually forms more than 90% of the overall two-phase pressure drop [28]. As the drift flux model gives very good predictions of the void fraction for bubbly flow regimes, the gravitational component of the overall two-phase pressure gradient is estimated using the model, based on drift flux model, presented by Zuber and Findlay [29].

$$\left(\frac{\partial p}{\partial x}\right)_H = \left(\frac{g}{g_c}\right)\rho_m\,, \tag{31}$$

$$\rho_m = \alpha_g \rho_g + \left(1 - \alpha_g\right)\rho_l\,, \tag{32}$$

where ρ_m is the in-situ mixture density, calculated through gas void fraction, which estimated by multi fluid modelin each step of calculation. There are many empirical and semi-empirical correlations for predicting this parameter. Here, the gas void fraction was calculated via drift-flux model [29]. In general, the acceleration term in right-hand side of Eq. (22) could be neglected in the bubbly flow [8]. The frictional component can be roughly predicted by the correlation, suggested by Wallis [28].

$$\left(\frac{\partial p}{\partial x}\right)_F = \frac{2 f_m v_m^2 \rho_m}{g_c D}\,, \tag{33}$$

$$v_m = v_{sl} + v_{sg}\,, \tag{34}$$

where v_m, v_{sl} and v_{sg} are mixture, liquid and gas superficial velocity, respectively. p is the pressure, g is yhe acceleration due to gravity and g_c is the conservation factor, (32.2 lbm.ft/ft/s^2). The friction factor, f_m, was estimated from an empirical correlation reported by Chen [30].

4. BOUNDARY CONDITIONS

It is impossible to simulate the whole tubing with actual length of 2531 m. On the other hand, as fully developed flow was assumed at the outlet, the length of the tube should be considered long enough to have a fully developed profile at the outlet boundary. Therefore, only the lowest 15 meters of the well, at least 80D, is regarded using Behbahani et al. criterion [16]. Since the computational domain is symmetric around the center axis, the symmetry axis boundary condition was employed at the tubing string center line [16]. At the tubing walls no slip boundary condition coupled with the standard wall function for the turbulence model [31] was imposed. Uniform velocity inlets were employed as boundary conditions at the gas and oil inlets. The influence of the gravitational force on the flow was taken into account. The coarse mesh size was considered in a way, that the computational domain was divided into 320,000 cells. As can be seen in Fig. 2, a finer grid treatment was employed near the injection point. A typical grid, boundary conditions, and coordinates system (x–r) are shown in Fig. 2.

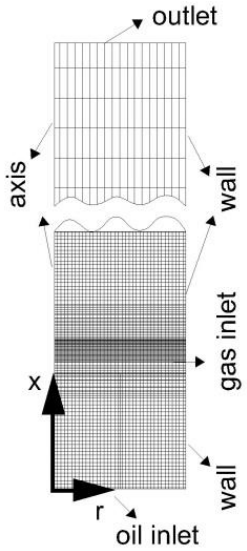

Fig. 2. The grid topology and boundary conditions.

5. MATERIALS AND METHODS

The two-dimensional (vertical) model was used to study the unsteady behaviour of two-phase fluid in an oil well under gas lift. The calculations were performed with a time step of 0.01 s. The governing equations, which were derived assuming isothermal incompressible multiphase flow, along with the boundary conditions, have been integrated over a control volume. The subsequent equations have been discretized over the control volume, using a finite volume method to yield algebraic equations, which can be solved in an iterative manner for each time step. The conservation equations are solved by the segregate solver, using implicit scheme. The discretization form for all the convective variables were taken to be second order up winding. Here, the adopted PISOalgorithm introduced by Issa and Oliveira was used for the pressure-velocity coupling [24, 25]. The k–ε model with the modified coefficients by Behbahani et al. [17] was used to treat turbulence phenomena in both phases. In this study, the residual value of the mass, velocity components and volume fraction was considered as a convergence criterion. The numerical computation was considered converged, when the scaled residuals of these variables in the control volume lowered by four orders of magnitude.

6. MODEL VALIDATION AND COMPARISON

In order to investigate the validity of the multi fluid model, the calculated total pressure drops, as the most important characteristic of a two-phase flow, were compared with the experimental data. Of the 44 test data, 43 were reported by Dhotre and Joshi [32] and one was taken from Mahmudi and Sadeghi [5]. According to Dhotre and Joshi, data were taken in a way to cover a wide range of column diameter and gas velocity inlet for the bubbly flow regime. The statistical results were obtained using arithmetic average of percent deviation, APD, and standard deviation, SD.

$$APD = \frac{\sum_{i=1}^{n} PD_i}{n}\,, \tag{35}$$

$$SD = \sqrt{\frac{\sum_{i=1}^{n} (PD_i - APD)^2}{n-1}}\,, \tag{36}$$

$$PD = \frac{P_{BH,\,m} - P_{BH,\,c}}{P_{BH,\,m}} \times 100\,. \tag{37}$$

The results of statistical analysis, applied to all 44 test data are shown in Tables 2 and 3. The small values of APD and SD imply the good agreement between measured pressure drops and calculated ones. For example, the overall percent and

Table 2. Summary of data and comparison results

	Code	v_l (m/s)	v_g (m/s)	$\Delta p/\Delta l$ ‘ (Kpa/m)		PD
				Measured	Calculated	
Air–water	D	0.05	0.13	9.44	8.90	5.71
	D	0.05	0.21	10.35	10.13	2.05
	D	0.05	0.29	11.63	11.44	1.64
	D	0.05	0.37	12.21	11.97	1.95
	D	0.05	0.45	12.48	12.20	2.28
	D	0.09	0.13	8.92	8.09	9.24
	D	0.09	0.21	10.67	10.24	3.96
	D	0.09	0.29	11.15	11.12	0.3
	D	0.09	0.37	11.12	11.20	-0.73
	D	0.09	0.45	11.49	12.52	-9.00
	D	0.14	0.13	9.2	8.80	4.39
	D	0.14	0.21	9.02	8.98	0.37
	D	0.14	0.29	9.6	9.14	4.82
	D	0.14	0.37	9.74	9.74	0.01
	D	0.14	0.45	9.44	9.54	-1.06
	D	0.19	0.13	9.51	8.87	6.71
	D	0.19	0.21	9.55	8.70	8.86
	D	0.19	0.29	9.68	9.50	1.84
	D	0.19	0.37	10.34	9.99	3.29
	D	0.19	0.45	12.59	12.87	-2.16
Air–ethanol	D	0.05	0.13	9.29	8.77	5.67
	D	0.05	0.21	7.29	6.89	5.47
	D	0.05	0.29	6.88	6.89	-0.2
	D	0.05	0.37	8.14	8.11	0.38
	D	0.05	0.45	8.45	8.53	-1.02
	D	0.09	0.13	7.48	7.27	2.85
	D	0.09	0.21	7.98	7.73	3.16
	D	0.09	0.29	8.49	8.37	1.36
	D	0.09	0.37	8.17	8.16	0.06
	D	0.09	0.45	9.08	9.11	-0.41
	D	0.14	0.13	7.88	6.79	13.81
	D	0.14	0.21	7.52	7.19	4.42
	D	0.14	0.29	7.77	7.65	1.54
	D	0.14	0.37	10.07	10.39	-3.15
	D	0.19	0.13	7.63	7.08	7.26
	D	0.19	0.21	7.88	7.24	8.10
	D	0.19	0.29	8.17	8.05	1.39
	D	0.19	0.37	8.47	8.43	0.46
	D	0.19	0.45	8.95	8.80	1.62
Gas–liquid	M	2.48	3.41	9.53	10.01	-5.30

Code: D — Dhotre and Joshi [32]; M — Mahmudi and Sadeghi [5]

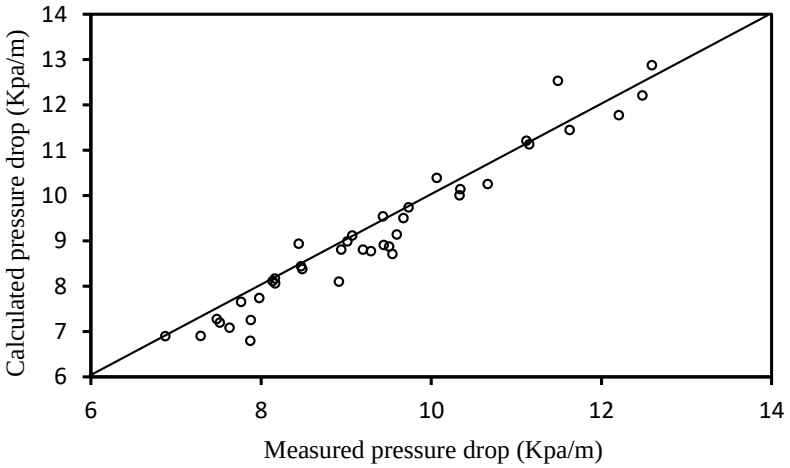

Fig. 3. Comparison of measured and calculated pressure gradient.

standard deviation values are 2.16 and 6.13 percent, respectively. It indicates, that if percent deviation is normally distributed about their mean value, the measured pressure drops would be predicted within ± 6.13 percent (l standard deviation) of the average percent difference. This statistical analysis is also exhibited graphically in Fig. 3. The results indicate the ability of the multi fluid model to predict pressure drop in the bubbly flow regime.

Table 3. Overall comparison results

Method	*APD*	*SD*
Multi fluid method	$+2.16$	6.13

7. Gas lift simulation

The multi fluid model was used to investigate the performance of gas lift in an oil well. The typical well, considered in this study, is located in one of the oil fields in the south of Iran. It started to produce light to medium crude oil in 1968. As time progressed, the reservoir pressure dropped as several wells did not flow naturally and were put on to gas lift. The study consists of a typical well tubing string with a diameter of 0.127 m and a length of 2531 m. The tubing contains crude oil, which hydrocarbon gas enters at the specific injection point. The computational domain is shown in Fig. 4. In addition, the properties of injected hydrocarbon gas are given in Table 4, while the relevant information and properties of the well and crude oil is illustrated in Table 5.

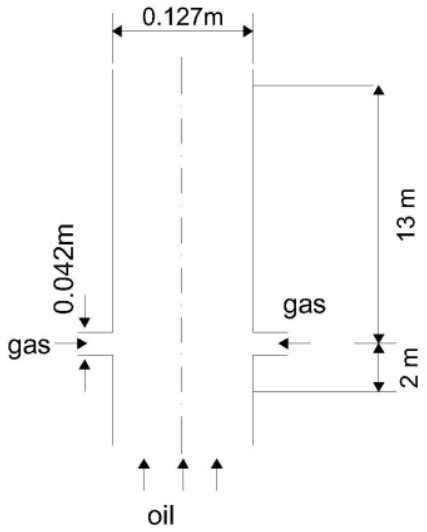

Fig. 4. The computational domain.

Table 4. Injected gas properties

Symbol	Definition	value
ρ_g	Density (kg/m^3)	145.60
v_g	Viscosity (Kg/m/s)	0.000202
Q_g	Gas injection rate (kg/s)	276.70
d	Bubble diameter (mm)	3

Table 5. Typical well information

Symbol	Definition	Value
BHP	Bottom hole pressure (Psi)	2920.15
T_{BH}	Reservoir temperature (°C)	92.59
T_{Top}	Surface temperature (°C)	27.86
GOR	Gas oil ratio (scf/bbl)	506
L	Length of tubing (m)	2531
D	Tubing inside diameter (m)	0.127
API	Oil API	30
ν_l	Viscosity of crude oil (cP)	0.207
WC%	Water cut	0.00
σ	Surface tension (N/m)	0.0086

8. RESULTS AND DISCUSSION

The performance of gas lift on the oil production is shown in Figs. 5 and 6. In these figures, the mixture density, superficial oil velocity and gas void fraction at different sections of the tubing are indicated. As it is obvious in these figures, at the gas injection point there is a turning point. When gas is injected, gas volume fraction increases significantly, so the fluid density decreases considerably at this point. In the bubbly flow regime, gravitational pressure drop is the dominant parts of the total pressure drop, therefore, the pressure gradient decreases significantly above the injection valve. It enables the BHP to accelerate the velocity of the flowing liquid vertically upward and increases oil production, as the oil velocity was increased to 0.29 m/s at the outlet. Also, it is shown in Fig. 6b that by pushing the oil, superficial oil velocity increases above the injected point.

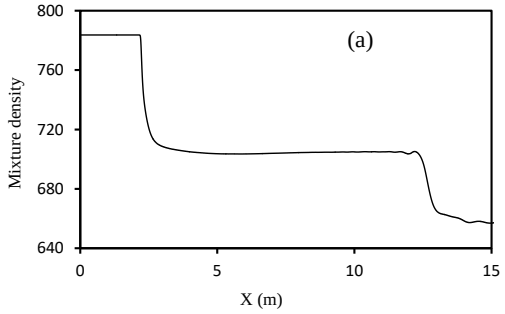

Fig. 5. The effect of injected gas on the mixture density and static pressure.

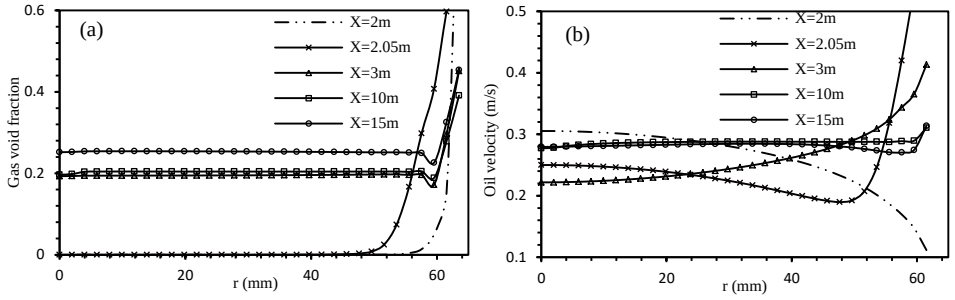

Fig. 6. The variation of gas void fraction (a) and oil superficial velocity (b) in the tubing.

The calculated gravitational pressure drop by multi fluid model was compared with those predicted by some empirical and semi empirical methods [8-12]. The best agreement belonged to the correlation introduced by Orkizevski by 0.41% average

error. The predictions by Kabir and Hasan and Aziz et al. were the same and relatively satisfactory by 3.30 and 3.63% error, respectively. The correlation developed by Chierici and Giucci by 6.25% error was in the next level. The worst prediction was by correlation introduced by Duns and Ros, which over predicted the gravitational pressure drop by large error up to 11%. It can be concluded, that the multi fluid model is able to predict pressure drop in oil wells with an acceptable accuracy.

8.1. Optimum operational condition

An optimal gas lift operation must justify three types of aims (i) maximization of produced oil, (ii) maximization of profit and (iii) optimization design of gas injection system. Generally, the effective parameters on the optimal gas lift process can be categorized on two important criteria. The first one is optimal operating parameters like position for injection point, tubing (or string) size and the way of injected gas distribution. The other one is estimating the optimal gas injection rate. As only the lower part of the tubing is simulated, the effect of the depth of injection point could not be discussed. However, the other parameters are investigated in the next section.

8.1.1. Effect of gas injection rate

The quantity of injected gas is one of the most important parameter, which directly affect the performance of gas lift. Figure 7 shows the variation of gas void fraction, oil superficial velocity and frictional pressure gradient in different axial distance from the injection point. The results concluded using bubbles with 3 mm diameter, as observed in Figs. 7a and 7b, the higher amount of injected gas, the larger gas void fraction near the wall and center of tubing. The density of the oil reduces by aerating the fluid resulting in lightening the two-phase flow fluid. According to Eq. (23), a lightened two-phase fluid developed less gravitational pressure drop, hence more amount of oil produced. It is clear in Fig. 7c, that the 24.5% increment in oil velocity is observed, when the gas injection rate is increased by 149.3%.

However, by increasing the amount of gas injected higher amount of fluid passes through tubing. As it can be notified in Eq. (25), higher mixture superficial velocity causes increasing the frictional pressure drop, accordingly (see Fig. 7c). The upward trend of frictional component results in decreasing the positive effect on oil production until reaching the economical optimum point (E.O.P.), where well fluid density reduction is equal to friction force increasing. At this point, the maximum quantity of well production is obtained. When the rate of injected gas keeps increasing, the reverse effect on production will be observed. Moreover, increasing the quantity of injected gas leads to increasing operational costs, which should be taken into consideration.

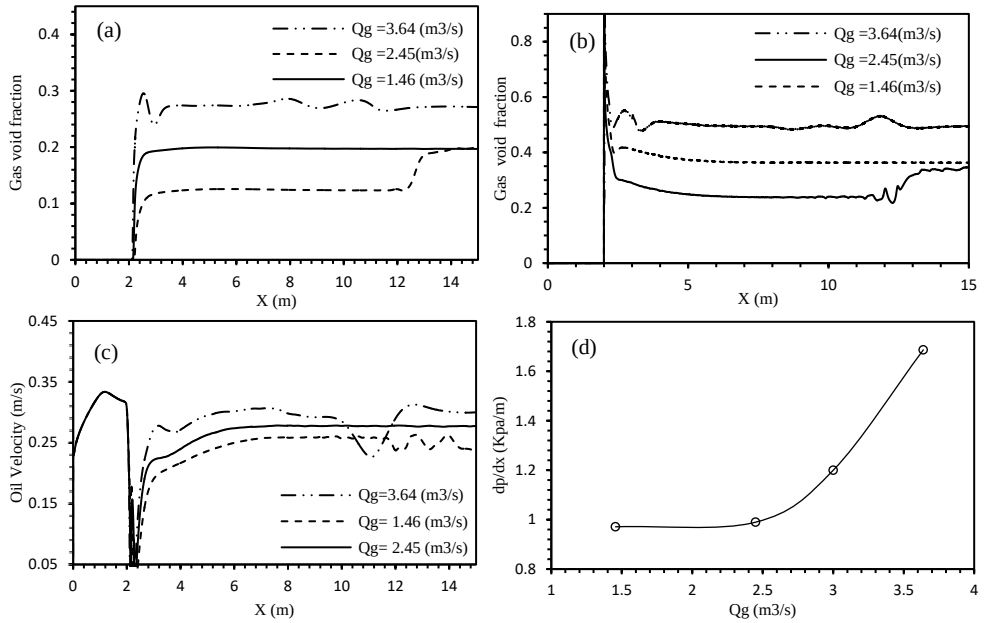

Fig. 7. The effect of the injected gas rate on the gas void fraction in center of tubing (a), near the wall (b) on the oil velocity (c) and frictional pressure drop (d).

8.1.2. EFFECT OF TUBING SIZE

Another parameter, which can significantly influence the performance of continues gas lift, is the size of tubing. The effect of tubing size is not simple and there are not apparent conclusions in literature. It considerably depends on flow rate and should be determined in each well particularly. Figure 8 involves the effect of tubing size on the pressure gradient, oil superficial velocity and gas void fraction. In this figure, the bubble diameter was assumed 3 mm and the quantity of injected gas was 2.45 m^3/s. Three standard tubing diameters with the size of 0.0706, 0.102 and 0.127 meters, regarding the operational limitations, are investigated. As observed in the following figure, by increasing the tubing size, gas void fraction, gravitational pressure, gradient and oil velocity in the center of tubing decrease. In fact, the frictional pressure drop increases, when the size of tubing diameter decreases. This increment of the frictional pressure drop overcomes the slight reduction of gravitational pressure drop.

8.1.3. EFFECT OF INJECTED GAS DISTRIBUTION

The bubble diameter is considered as a critical parameter to discuss the effect of the injected gas distribution on gas lift performance. All simulation was performed in a

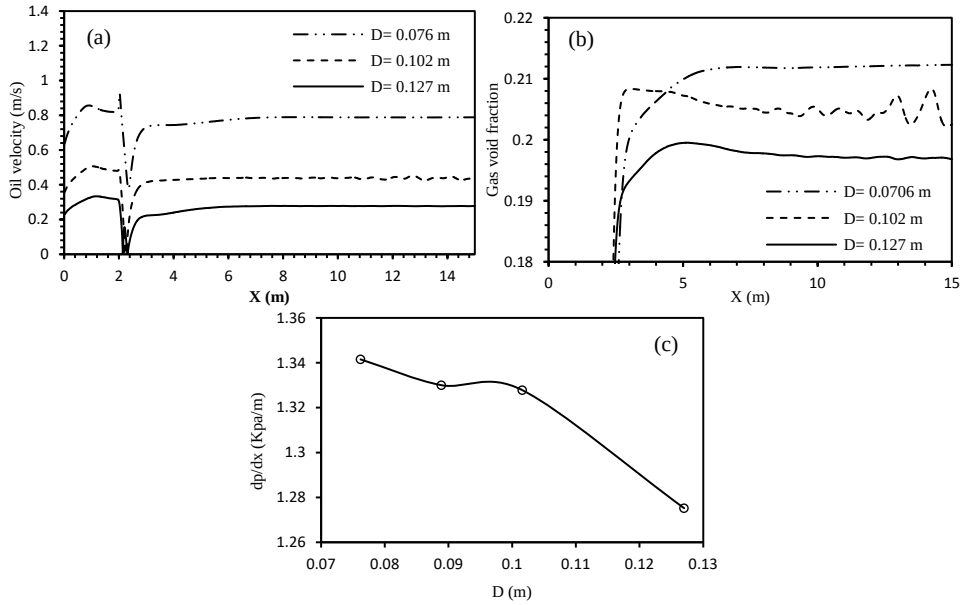

Fig. 8. The variation of gas void fraction: (a) oil superficial velocity, (b) gravitational pressure drop, (c) with tubing diameter.

constant gas injected rate equal to 24.50 m^3/s. Figure 9 illustrates the gravitational pressure gradient, gas void fraction and oil superficial velocity in different size of bubble diameter. It can be seen in Fig. 9a, decreasing the bubble size causes increasing gas void fraction in the center of the pipe and successively decreasing it near the wall. So, the smaller bubbles improve gas distribution in the tubing. Also, it is shown in Figs. 9b and 9c, when the smaller bubbles were injected, gravitational pressure drop decreased and higher oil velocity were observed in the tubing.

9. CONCLUSION

In this study, the gas lift process in a typical well in one of the oil fields in the south of Iran was simulated. A multi fluid model, based on CFD technique was developed to study the behaviour of two-phase flow in the vertical pipe. A statistical analysis was conducted and the accuracy of the multi fluid model was investigated. The results showed that the proposed method, performed reasonably well to predict the complex behaviour of two-phase flow. The model was used to investigate the performance of gas lift around the injection point in an oil well under gas lift. The calculated pressure drop was compared with those predicted by other empirical and semi empirical models. The low values of errors showed the accuracy of the model to simulate gas

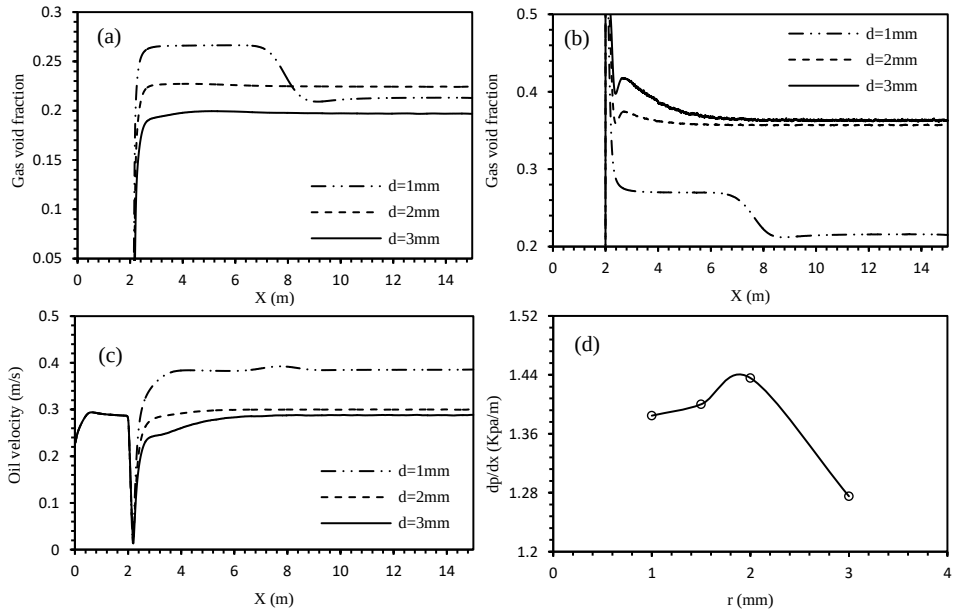

Fig. 9. The influence of bubble diameter on gas void fraction in the center of tubing (a), near the wall (b), on oil superficial velocity (c) and gravitational pressure drop (d).

lift for the other wells in the oil field. In addition, the results showed that injection of gas raised the oil velocity up to 0.29 m/s at outlet.

The multi fluid model then was used to survey the effect of the operational parameters including tubing size, injected gas distribution and the rate of injected gas on the performance of gas lift. The results revealed the sensitivity of the continuous gas lift to its design and operational parameters. The oil production rate was increased by decreasing bubble size as well as increasing the injected gas rate. As oil velocity rose by 24.5%, the gas injected rate was increased by 149.3%. However, the effect of tubing size is more complicated. For the considered well in this study, increasing the tubing size declined oil superficial velocity, which caused to decrease oil production.

REFERENCES

[1] TAKACS, G. Gas Lift Manual, Tulsa, Penn Well, 2005.

[2] MAYHILL, T. D. Simplified Method for Gas Lift Well Problem Identification and Diagnosis, SPE 5151, SPE 49th Annual Fall Meeting Houston, USA, Texas, October 6-9, 1974.

[3] GOMEZ, V. Optimization of Continuous Flow Gas Lift Systems, M. S. Thesis, USA, Oklahoma, Tulsa, 1974,

[4] KANU, E. P., J. MACH, K. E. BROWN. Economic Approach to Oil Production and Gas Allocation in Continuous Gas Lift. *J. Pet. Technol.*, **10** (1981), No. **3**, 1887-1892.

[5] MAHMUDI, M., M. T. SADEGHI. The Optimization of Continuous Gas Lift Process using an Integrated Compositional Model. *J. Pet. Sci. Eng.,* **108** (2013), 321–327.

[6] FANG, W. Y., K. K. LO. A Generalized Well Management Scheme for Reservoir Simulation. *SPE Reserv. Eng.,* **11** (1996), 116-120.

[7] ALARCON, G. A., C. F. TORRES, L. E. GOMEZ. Global Optimization of Gas Allocation to a Group of Wells in Artificial Lifts Using Nonlinear Constrained Programing. *J. Energy Resour. Technol.*, **124** (2002), 262-268.

[8] KABIR, C. S., A. R. HASAN. Performance of a Two-phase Gas/Liquid Flow Model in Vertical Wells. *J. Pet. Sci. Eng.*, **4** (1990), 273–289.

[9] ORKISZEWSKI, J. Predicting Two-phase Pressure Drops in Vertical Pipes. *J. Pet. Technol.*, **19** (1967), No. **6**, 829–838.

[10] AZIZ, K., G. W. GOVIER, M. FOGARASI. Pressure Drop in Wells Producing Oil and Gas. *J. Can. Petrol. Technol.,* **11** (1972), 38–47.

[11] CHIERICI, G. L., G. SCLOCCHI. Two-Phase Vertical Flow in Oil Wells - Prediction of Pressure Drop. *J. Pet. Technol.*, **26** (1974), No. 8, 927–938.

[12] DUNS, JR. H., N. C. J. ROS. Vertical Flow of Gas and Liquid Mixtures in Wells, In: Proc. 6th World Petroleum Congress, Germany, Frankfurt am Main, 19-26 June, 1963, 451–465.

[13] TROSHKO, A. A., Y. A. HASSAN. A Two-equation Turbulence Model of Turbulent Bubbly Flows. *Int. J. Multiph. Flow.*, **27** (2001), 1965–2000.

[14] LAMB, H. Hydrodynamics, New York, Cambridge University Press, 1932.

[15] DREW, D. A., R. T. LAHEY JR. Application of General Constitutive Principles to the Derivation of Multidimensional Two-phase Flow Equation. *Int. J. Multiph. Flow*., **5** (1979), 243–264.

[16] BEHBAHANI, M. A., M. EDRISI, F. RASHIDI, E. AMANI. Tuning a Multi-Fluid Model for Gas Lift Simulations in Wells. *Chem. Eng. Res. Des.,* **90** (2011), No. **4**, 471–486.

[17] ISHII, M., N. ZUBER. Drag Coefficient and Relative Velocity in Bubbly, Droplet or Particulate Flows. *AIChE J.,* **25** (1979), 843–855.

[18] SCHILLER, L., A. NAUMANN. A Drag Coefficient Correlation. *V. D . I. Zeitung*, **77** (1935), 318–320.

[19] TOMIYAMA, A. Struggle with Computational Bubble Dynamics. *Multiph. Sci. Technol.*, **10** (1998), No. **4**, 369-405.

[20] FRANK, TH., P. J. ZWART, E. KREPPER, H. M. PRASSER, D. LUCAS. Validation of CFD Models for Mono- and Polydisperse Air–Water Two-phase Flows in Pipes. *Nucl. Eng. Des.,* **238** (2008), 647–659.

[21] GUET, S., G. OOMS. Fluid Mechanical Aspects of the Gas-lift Technique. *Annu. Rev. Fluid Mech*., **38** (2006), 225–249.

[22] HARLOW, F. H., P. I. NAKAYAMA. Transport of Turbulence Energy Decay Rate, Los Alamos Scientific Laboratory report LA-3854, 1968.

[23] BELF'DHILA, R., O. SIMONIN. Eulerian Predictions of a Turbulent Bubbly Flow downstream a Sudden Pipe Expansion, In: Sommerfeld, M. (Ed.), Sixth Workshop on Two-Phase Flow Predictions, Germany, Erlangen, 1992.

[24] ISSA, R. L. Solution of the Implicitly Discretized Fluid Flow Equations by Operator Splitting. *J. Comp. Phy.,* **62** (1986), 40-65.

[25] ISSA, R. L, P. J. OLIVEIRA. On The Numerical Treatment of Interphase Forces in Two-phase Flow. *Numer. Methods Multiphase Flows*, **185** (1994), 131-140.

[26] BEHZADI, A., R. L. ISSA, H. RUSCHE. Modeling of Dispersed Bubble and Droplet Flow at High Phase Fractions. *Chem. Eng. Sci.*, **59** (2004), 759-770.

[27] ISSA, R. L, P. J. OLIVEIRA. Numerical Prediction of Phase Separation in Two-phase Flow through T-junctions. *Comput. Fluids,* **23** (1993), No. **2**, 347-372.

[28] WALLIS, G. B. One Dimensional Two-Phase Flow, New York, McGraw-Hill, 1969.

[29] ZUBER, N., J. A. FINDLAY. Average Volumetric Concentration in Two-phase Flow Systems. *J. Heat Transfer. Trans.,* ASME, **83** (1965), 453-468.

[30] CHEN, N. H. An Explicit Equation for Friction Factor in Pipe. *Ind. Eng. Chem. Fundam.*, **18** (1997), No. **3**, 296-297.

[31] LAUNDER, B. E., D. B. SPALDING. The Numerical Computation of Turbulent Flows. *Comput. Method Appl. Mech. Eng.,* **3** (1974), 269–289.

[32] DHOTRE, M. T., J. B. JOSHI. Two-dimensional CFD Model for the Prediction of Flow Pattern, Pressure Drop and Heat Transfer Coefficient in Bubble Column Reactors. *Chem. Eng. Res. Des.*, **82** (2004), 689–307.